Alexandria Engineering Journal (2015) 54, 993–1002

HOSTED BY

Alexandria University

Alexandria Engineering Journal

www.elsevier.com/locate/aej
www.sciencedirect.com

ORIGINAL ARTICLE

Validation of some engine combustion and emission parameters of a bioethanol fuelled DI diesel engine using theoretical modelling

Murugan Sivalingam [a,b,*], Subranshu Sekhar Mahapatra [b], Dulari Hansdah [b], Bohumil Horák [a]

[a] Department of Cybernetics and Biomedical Engineering, VSB Technical University, Ostrava, Czech Republic
[b] Department of Mechanical Engineering, National Institute of Technology, Rourkela, India

Received 10 June 2015; revised 19 August 2015; accepted 1 September 2015
Available online 19 October 2015

KEYWORDS

Compression ignition (CI) engine;
Madhuca Indica flower;
Bioethanol;
Mathematical modelling;
MATLAB

Abstract Earlier reports indicate that ethanol/bioethanol can replace conventional diesel fuel by 15%, when it is emulsified with diesel and used as an alternative fuel in a compression ignition (CI) engine. In this study, initially BMDE15, a bioethanol emulsion containing 15% bioethanol, 84% diesel and 1% surfactant was characterised for its fuel properties and compared with those of diesel fuel properties. The numerical value indicates the percentage of bioethanol in the BMDE15 emulsion. For the investigation, bioethanol was obtained from the Mahua Indica flower which was collected from the Madhuca Indica tree, and it was produced from fermentation process using *Saccharomyces cerevisiae*. Further, the BMDE15 emulsion was tested in a single cylinder, four stroke, air cooled, DI diesel engine developing a power of 4.4 kW at a rated speed of 1500 rpm. Two important combustion parameters: cylinder pressure and ignition delay, and two important emission parameters: nitric oxide (NO) and smoke emissions were determined and compared with those of diesel operation at all loads. The experimental results were validated using mathematical modelling, and the analysis of the results is presented in this paper.

1. Introduction

Ethanol is considered to be a potential alternative fuel for transport applications. It can be derived from a variety of sources. Although ethanol has been used in the form of a blend with gasoline, in spark ignition (SI) engines in the last three decades, the use of ethanol in compression ignition (CI) engines is of more interest because of the wider acceptance of CI engines in many applications [1]. Ethanol derived from biomass materials known as bioethanol is paid more attention because it can be derived from a variety of biomass materials which are renewable and abundantly available [2,3]. Numerous research works have been documented to use in the form of blending/emulsion, fumigation, dual injection, surface ignition,

* Corresponding author at: Department of Cybernetics and Biomedical Engineering, VSB Technical University, Ostrava, Czech Republic. Tel.: +420 702959180/+91 661 2462525
E-mail address: muruganresearch@yahoo.com (M. Sivalingam).
Peer review under responsibility of Faculty of Engineering, Alexandria University.

http://dx.doi.org/10.1016/j.aej.2015.09.003

etc. in CI engines [4]. In recent years the study and control of emissions from internal combustion (IC) engines have been highly concentrated.

Theoretical analysis accomplished by mathematical modelling or numerical solutions using computer program or computational fluid dynamics (CFD) can give more fruitful predictions on the engine parameters [5]. The simulation model by MATLAB program for numerical solution was used to analyse the engine parameters of a single cylinder 3.5 kW rated power diesel engine fuelled with diesel, Palm Oil Methyl Ester and POME-diesel blends [6]. The results reported that, the simulated results on the brake thermal efficiency and in-cylinder pressure were closer by about 2–3% to the experimental results. A single-zone thermodynamic model was developed for a diesel engine fuelled with biodiesel from waste [6]. The single zone model coupled with a triple-Wiebe function was performed to simulate heat release and cylinder pressure. It was reported that, the heat release rate and cylinder pressure predicted were 2.5% and 2.2% closer to the experimental results of the engine. A two dimensional, multi-zone model was developed for a DI diesel engine run with the ethanol–diesel blend [7] and vegetable oil, bio-diesel and diesel [8]. The simulation model was supported by Fortran V language and solved numerically by solution marching technique with a computational step size of 1° crank angle. The heat transfer formulations used in a diesel engine under different operating conditions were computed using computational fluid dynamics (CFD) codes [9] was evaluated and compared with the experimental data. The model predicted more accurately the heat transfer during the compression stroke for motored operation and at the same time the predicted peak heat flux was closer to the experimental results. A quasi-dimensional, multi-zone, direct injection (DI) diesel combustion model has been developed and implemented in a full cycle simulation of a turbocharged engine. Predictions of heat release rate, as well as NO and soot emissions are compared with experimental data obtained from representative heavy-duty, turbocharged diesel engines. It is demonstrated that the model can predict the rate of heat release and engine performance with high fidelity. However, additional effort is required to enhance the fidelity of NO and soot predictions across a wide range of operating conditions [10]. A quasi-dimensional, three-zone combustion model of the diesel engine to calculate performance and emissions using the diesel–ethanol dual fuel was developed by Juntarakod [11]. A study was carried out using multizone modelling to analyse the spray development of a diesel engine run on vegetable oil, and biodiesel diesel blends [12]. It was reported that the prediction of results from modelling was more proximate than the experimental results. The computational time required was not affected in the multi-dimensional modelling. The combustion model of a diesel engine was developed using computational fluid dynamics (CFD) software-AVL Fire, and the performance and emission characteristics for second generation biodiesel were analysed [13]. The simulated results reported that, biodiesel provided better performance and efficiency, and significantly reduced engine emissions. The quasi-dimensional, multi-zone (QDMZ) models [14,15] were formulated by the quasi steady equations which described the individual processes that occur in the engine cylinder such as fuel atomisation, fuel injection, air entertainment, air–fuel mixing, combustion and heat transfer. A combustion model [16,17] was developed for the theoretical DI diesel engine and performance parameters. It was reported that the developed model could be adapted for an alternative fuel in a diesel engine and the performance and cylinder pressure results were closer to the theoretical.

In recent years, the validation of the experimental results from mathematical modelling or simulation through advance software is essential, so that the randomness of the results is minimised. In this study, a mathematical modelling was developed to validate the experimental results obtained from a single cylinder, four stroke, air cooled, DI diesel engine, that was run on the BMDE15 emulsion. A MATLAB program was developed for a two zone model for the validation. One zone consisted of pure air called the non-burning zone, and the other consisted of fuel and combustion products, called the burning zone. In order to obtain the cylinder pressure and temperature by mathematical modelling, the first law of thermodynamics and the equation of state were used for both the zones. The combustion parameters, such as ignition delay and heat release rate the chemical equilibrium composition were calculated theoretically, using the two zone model. As the NO and soot emissions are important in a CI engine, they were calculated using a semi-empirical model. A comparison of the theoretical and experimental results of the BMDE15 emulsion is presented in this paper. A spray profile of diesel and the BMDE15 emulsion is also obtained using a MATLAB program and is presented.

2. Materials and method

In this experimental investigation, bioethanol obtained from the Madhuca Indica flower and emulsified with diesel (BMDE15) was used as an alternative fuel in a single cylinder, four stroke, direct injection (DI) diesel engine. Table 2 lists the important properties of diesel and BMDE15. The complete procedure of producing the bioethanol from the Madhuca Indica flower has already been described in [18]. The numeric value after BMDE indicates the percentage of bioethanol in the emulsion. The physicochemical properties of the BMDE15 emulsion are shown in Table 1 in comparison with those of diesel.

The experimental set-up used in this investigation is shown in Fig. 1. A series of tests were carried out on a single cylinder, air cooled, stationary DI diesel engine that has a bore diameter of 87.5 mm and a stroke length of 110 mm and a displacement of 662 cm. The engine had a rated output of 4.4 kW 1500 rpm with a compression ratio 17.5:1. The nozzle opening pressure of the injector was 200 bar and the injection timing was 23 °CA bTDC, set by the manufacturer.

The engine was coupled to an electrical dynamometer to provide the brake load with an electric panel. Diesel and

Table 1 Properties of diesel and BMDE15.

Description	Diesel	BMDE15
Chemical formula	$C_{16}H_{34}$	$C_{5.471}H_{6.039}O$
Molecular weight	170	48
Viscosity at 40 °C, cSt	2.4	1.73
Carbon	86	65.65
Hydrogen	13.60	10.21
Nitrogen	0.18	0.14
Sulfur	0.22	0.01
Oxygen by difference	0	24

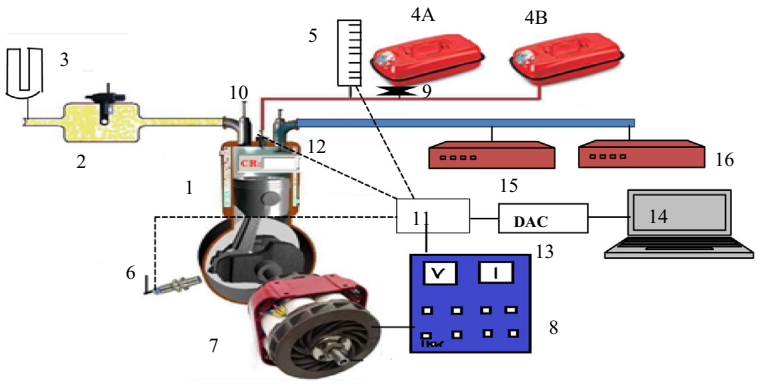

1. Engine
2. Air box
3. U-tube Manometer
4A.Diesel tank
4B.Emulsion tank
5. Burette
6. Crank angle encoder
7. Alternator
8. Load cell
9. Valve
10. Fuel injector
11. Control panel
12. Pressure transducer
13. Data acquisition card
14. Personal computer
15. AVL437C smoke meter
16. AVL Digas 444 analyser

Figure 1 Experimental set-up.

Table 2 Important properties of diesel and BMDE15.

Properties	ASTM standard	Diesel	BMDE15
Density at 40 °C (kg/m^3)	D4052-11/ D4815	860	809
Lower heating value (MJ/kg)	D 4809	43.8	35.34
Kinematic viscosity at 40 °C (cSt)	D 445	2.58	1.95
Cetane number	D613	51	36
Flash point (°C)	D 2500	52	26

BMDE15 emulsion were stored in two different fuel tanks, respectively. A fuel control valve was located in the fuel line between diesel tank and alternative fuel tank, to allow either diesel or emulsion fuel. The fuel consumption was measured with the help of a fuel sensor, which was fixed in the fuel line. The emulsion was injected by the fuel injector of the system. An air box was provided on the suction side of the air. Air consumption was measured with the help of air sensor which is fitted on the air box. The exhaust gas temperature measured by a K type thermocouple and input were given to the data acquisition system. The data collected by the data acquisition system from all the sensors for the corresponding loads were displayed on the monitor of the computer. A water cooled piezo-electric pressure transducer with a sensitivity of 12.5 pC/bar, was mounted on the cylinder head. A TDC position sensor was fixed on the flywheel of the engine. The pressure transducer and the TDC position sensor gave the input to the data acquisition system. With the help of the pressure measured at every crank angle, pressure–crank angle diagram was drawn. For the emission measurements, an exhaust gas analyser was used to measure the level of HC, CO_2, CO, and NO. A diesel smoke meter was used to measure the smoke in the engine exhaust. Initially, the engine was operated with diesel for obtaining the reference data.

3. Mathematical modelling

3.1. Fuel model

3.1.1. Spray formation model

In a CI engine, the fuel air mixture is obtained inside the combustion chamber of the engine. The injected fuel absorbs the heat from the surrounding air and vapourises. Further, the fuel vapour mixes with the available air in the cylinder. The fuel injector plays an important role in the injection process, because it atomises the liquid fuel into finer droplets in the form of a spray. Depending on the spray, the fuel air mixture is obtained in the cylinder. The better the fuel spray, the better the mixture formation. The combustion, performance and emission of the engine are analysed with the help of a spray pattern of the fuel. In this section, the two-dimensional, multi-zone model of fuel sprays is developed, where the issuing jet is divided into discrete volumes, called zones. The descriptions of the model are discussed in the following subsections.

3.1.2. Fuel injection process

During the compression of fluid in the fuel injection process, a pressure wave is propagated down the connecting pipe at a sonic speed, to open the needle of the injector. The speed of sound is given by

$$a_s = \sqrt{\frac{K_{bm}}{\rho_1}} \tag{1}$$

Then, the time for the pressure wave to travel down the connecting pipe length (L_p) i.e. injection delay was expressed by

$$\Delta\varphi_{injdel} = \left(\frac{L_p}{a_s}\right)6N \tag{2}$$

The pressure wave in the injector nozzle holes has a magnitude of

$$\Delta p_w = a_s \rho_1 c_{pump}\left(F_{pump}/F_{nozzle}\right) \tag{3}$$

where F_{pump} and F_{nozzle} are the cross sectional areas of the pump barrel and of the total of the nozzle holes.

3.1.3. Fuel jet break-up point and initial angle

To obtain the location of the spray tip as a function of time, based on the relevant experimental data and turbulent jet theory, a correlation developed by Arai et al. [19] is incorporated in the modelling. Other correlations [20,21] are also used to obtain the fuel break-up point, swirling motion of the air and spray penetration containing the swirl ratio.

The mean jet velocity from each nozzle hole is given by

$$\bar{u}_{inj} = C_d\sqrt{2\overline{\Delta p}_{inj}/\rho_1} \tag{4}$$

The C_d value was taken as 0.39.

The mean fuel injection rate per jet (kg/°CA) is given as

$$\acute{m}_{finj} = \left(\pi D_n^2/4\right)\rho\bar{u}_{inj}/6N \tag{5}$$

For the given global air to fuel ratio, the total fuel mass to be injected in the cycle m_{ftot} is fixed, if the total air mass trapped in the cylinder m_{atot} is known. Then, the value of the total duration of the fuel injection is given in degrees of the crank angle,

$$\Delta\varphi_{inj} = \left(m_{ftot}/Z\right)/\acute{m}_{finj} \tag{6}$$

The spray development will continue until the penetration of each spray reaches a value of $(D/2 + \pi D/z)$, or until it entrains the maximum quantity of air equal to m_{atot}/z.

The break-up time t_{br} was obtained by equating the two spray penetration correlations before and after t_{br}, corresponding to the break-up length $S = S_{br}$

$$S = 0.39\sqrt{2\overline{\Delta p}_{inj}/\rho_1 \cdot t} \quad \text{for } 0 < t \leqslant t_{br} \tag{7}$$

$$S = 2.95\left(\overline{\Delta p}_{inj}/\rho_a\right)^{0.25}\sqrt{D_n \cdot t} \quad \text{for } t \geqslant t_{br} \tag{8}$$

Then t_{br} is given by

$$t_{br} = 28.61\rho_1 \cdot D_n \Big/ \sqrt{\rho_a \cdot \overline{\Delta p}_{inj}} \tag{9}$$

where ρ_a is the density of air inside the cylinder just before the beginning of the combustion of fuel.

The break-up length is given as

$$S_{br} = \bar{u}_{inj} \cdot t_{br} \tag{10}$$

The break-up length with the swirl ratio can be written as

$$S_{brs} = S_{br}\left(1 + \pi \cdot R_s \cdot N \cdot S_{br}/30 \cdot \bar{u}_{inj}\right)^{-1} \tag{11}$$

The corresponding break-up time is given by

$$t_{brs} = S_{brs}/\bar{u}_{inj} = (S_{brs}/S_{br}) \cdot t_{br} \tag{12}$$

The initial spray angle (rad) is [22]

$$\theta = 2\arctan\left(\frac{1}{\acute{A}}4\pi\sqrt{\frac{\rho_a}{\rho_1}}\frac{\sqrt{3}}{6}\right) \tag{13}$$

where $\acute{A}$ is constant and given by the empirical relations,

$$\acute{A} = 3 + 0.28(L_n/D_n) \tag{14}$$

3.1.4. Fuel spray development

The following steps are used for the spray development of each zone,

(a) For axial zones, the zones are taken as $i_{max} = \Delta\varphi_{inj}/\Delta\varphi$, and for radial zones, they are divided into $j_{max} = i_{max}/2$ to i_{max}. The instantaneous fuel injection velocity and injection rate in each spray, using instantaneous values of $\Delta p_{inj} = \Delta p_w$ are given as

$$u_{inj}(i) = C_d\sqrt{2\overline{\Delta p}_{inj}(i)/\rho_1} \tag{15}$$

And

$$\acute{m}_{finj}(i) = \left(\pi D_n^2/4\right)\rho u_{inj}(i)/6N \tag{16}$$

Then the cumulative fuel injected in each spray is,

$$m_{finj}(i) = \int_0^{\varphi} \acute{m}_{inj}(i)d\varphi \tag{17}$$

(b) The fuel is distributed equally into the radial zones j_{max} at each crank angle in steps of "i", which is given by the following equation,

$$m_{finj}(i) = \acute{m}_{inj}(i)d\varphi/j_{max} \tag{18}$$

(c) The Sauter mean diameter (D_{SM}) is calculated for each step.

(d) The mid zone is selected as

$$j_{mid} = j_{max}/2 + 1 \tag{19}$$

(e) The mid-zone penetration in the radial distance from the cylinder axis is calculated as

$$r_{mid}(i) = \sqrt{x^2(i,j_{mid}) + y^2(i,j_{mid})} \tag{20}$$

(f) The mid-zone velocity in each crank angle step (i) is calculated as

$$u_{mid}(i) = 2.95\beta\left(\Delta p_{inj}(i)/\rho_a\right)^{0.25}\sqrt{D_n}\frac{1}{t^{1-\beta}} \tag{21}$$

(g) The centre line angle for each zone is given as

$$\theta_z(i,j) = -\frac{\theta}{2} + \frac{j-1}{j_{max}}\theta + \frac{\theta}{2j_{max}} \tag{22}$$

(h) The velocity distribution for a lower axis penetration located at the jet periphery for each zone is calculated as

$$u_z(i,j) = u_{mid}(i)\exp\left[-\alpha\theta_z^2(i,j)\right] \tag{23}$$

where $\alpha = 4.5^2$

(i) The swirl coefficient before the wall impingement is calculated by the following equation,

$$C_{swz}(i,j) = 1 + \frac{\pi R_n N\sqrt{x^2(i,j_{mid}) + y^2(i,j_{mid})}}{30u_z(i,j)} \tag{24}$$

while $C_{swz}(i,j)$ is 1 after the wall impingement. The coordinates of x and y are calculated from the previous step.

(j) Also the drop of the Sauter mean diameter from the centre line of the spray with increasing distance is considered as

$$D_{SM}(i,j) = \left(1 - \frac{1}{w}\right) D_{SMM}(i) + \left(\frac{2}{w}\right) D_{SMM}(i)(j-1)/(j_{mid} - 1) \tag{25}$$

where w is in the range of 5–10.

(k) The number of droplets in each zone is also calculated with the following mathematical relation:

$$N_{drop}(i,j) = m_{fz}(i)/[(\pi/6)] D_{SM}(i,j)^3 \rho_1] \tag{26}$$

(l) The zone velocity with swirl is calculated as

$$u_{zs}(i,j) = u_z(i,j)/C_{swz}(i,j) \tag{27}$$

(m) The mass of air in each zone is calculated as

$$m_{az}(i,j) = m_{fz}(i) \frac{u_{inj}(i) - u_{zs}(i,j)\cos\theta_z(i,j)}{u_{zs}(i,j)\cos\theta_z(i,j)} \tag{28}$$

(n) The fuel air equivalence ratio of the zone is,

$$\varnothing_z(i,j) = \frac{m_{fz}(i)/m_{az}(i,j)}{\left(\frac{1}{AF_{st}}\right)} \tag{29}$$

(o) The effect of swirl for each zone on the angle is considered as

(i) For $j < j_{mid}$,

$$\theta_{zs}(i,j) = \theta_z(i,j) C_{swz}(i,j)^2 \tag{30}$$

(ii) For $j = j_{mid}$,

$$\theta_{zs}(i,j_{mid}) = \frac{1}{2}\theta_{zs}(i,j_{mid}) + \frac{1}{2}\theta_{zs}(i,j_{mid} - 1) \tag{31}$$

(iii) For $j > j_{mid}$,

$$\theta_{zs}(i,j) = \theta_z(i,j) + \theta_{zs}(i,j_{mid}) \tag{32}$$

(p) The location of the co-ordinates for each zone is calculated with the following equation:

(i) Before the wall impingement,

$$x(i,j) = x_0(i,j) + u_{zs}(i,j)\cos\theta_{zs}(i,j)\frac{\Delta\varphi}{6N} \tag{33}$$

$$y(i,j) = y_0(i,j) + u_{zs}(i,j)\sin\theta_{zs}(i,j)\frac{\Delta\varphi}{6N} \tag{34}$$

(ii) After the wall impingement,

$$x(i,j) = r_{zimp}(i,j)\cos\theta_{zs}(i,j) \tag{35}$$

$$y(i,j) = r_{zimp}(i,j)\sin\theta_{zs}(i,j) \tag{36}$$

3.1.5. Fuel droplet evaporation

The fuel evaporation in each zone is considered with the calculation of the Sauter mean diameter, which is given by the following relations:

$$D_{SM,1} = 0.38 Re_{inj}^{0.25} We_{inj}^{-0.32} (v_1/v_a)^{0.37} \left(\frac{\rho_1}{\rho_a}\right)^{-0.47} D_n \tag{37}$$

$$D_{SM,2} = 4.12 Re_{inj}^{0.12} We_{inj}^{-0.75} (v_1/v_a)^{0.45} \left(\frac{\rho_1}{\rho_a}\right)^{0.18} D_n \tag{38}$$

Also, the equivalence ratio for each zone is calculated using the evaporation model,

$$\varnothing_{zvap}(i,j) = \frac{m_{fzvap}(i)/m_{az}(i,j)}{\left(\frac{1}{AF_{st}}\right)} \tag{39}$$

3.1.6. Calculation of Whitehouse–Way fuel preparation rate constant

After the fuel is injected into the cylinder chamber, it will undergo physical and chemical processes for burning inside the chamber. In the physical process, the fuel gets atomised, heated, evaporated and mixed with sufficient air to form the charge mixture. Then, the chemical kinetic reactions occur, to burn the mixture in the chemical process. The Whitehouse and Way model [23] was used for the comparison of the results obtained from the fuel evaporation model. So, the penetration rate proposed by the Whitehouse–Way model was given as

$$\frac{dm_{pr}}{d\varphi} = K_{pr} m_{inj}^{1-x} m_{fup}^{x} p_{ox}^{m} \tag{40}$$

where

$$m_{finj} = \int_0^{\varphi} \frac{dm_{finj}}{d\varphi} d\varphi \tag{41}$$

$$m_{fup} = m_{finj} - \int_0^{\varphi} \frac{dm_{finj}}{d\varphi} d\varphi \tag{42}$$

3.2. General description of the model

In this investigation, a single cylinder, four stroke, air cooled, direct injection (DI) diesel engine is used. The combustion chamber is a bowl in piston type and the fuel injector has a three hole nozzle. The model used in this study is a two zone thermodynamic model. It is assumed that the cylinder contains a nonburning zone of air, and another burning zone in which the fuel is continuously injected during injection and burnt with the available air from the air zone. The model considers only those processes which occur during the possession of compression and expansion stroke. It is assumed that the inlet and exhaust valves are fully closed during the stroke. The compression process in practically all engines is a polytropic one, which begins from the moment the inlet valve, closes and ends when the injection process starts. The main calculation is based on the integration of the first law of thermodynamics and the ideal gas equation. The following assumptions are made for the analysis:

(a) The cylinder contains the non-burning zone and burning zone.

(b) The pressure and temperature in each zone are uniform and vary with the crank angle. The content of each zone follows the perfect gas laws.

3.2.1. Energy equations

During the compression stroke, only one zone (of pure air) exists. Then, the first law of thermodynamics for a closed system is applied, together with the perfect gas state equation. The change in internal energy is expressed [21] as follows:

$$\frac{d(mu)}{d\theta} = \frac{dQ_r}{d\theta} - \frac{dQ_h}{d\theta} - \frac{dW}{d\theta} \tag{43}$$

By replacing the work transfer term $dW/d\theta$ with $PdV/d\theta$ or by the ideal gas law $PV = mRT$, the above Eq. (43) can be rearranged as

$$m\frac{du}{d\theta} = \frac{dQ_r}{d\theta} - hA\frac{dT}{d\theta} - RT\frac{dV}{d\theta} \tag{44}$$

where V is the instantaneous cylinder volume with respect to the crank angle, which is given by

$$V = V_{cl} + (\pi D^2/4)r\left[1 + \lambda^{-1} - \cos\varphi - \left(\lambda^{-2} - \sin^2\varphi\right)^{1/2}\right] \tag{45}$$

In the above equations, the term dQ is given as the fourth order polynomial expression of the absolute temperature T, including the enthalpy of formation at absolute zero.

The internal energy calculation as a function of temperature is as follows:

$$\frac{hi}{R_{mol}T} = ai1 + ai2/2T + ai3/3T^2 + ai4/4T^3 + ai5/5T^4 + ai6/3T^5 \tag{46}$$

$$ui = hi - RT \tag{47}$$

For the surrounding air zone, which only loses the mass (air) to the burning zone, the first law of thermodynamics for the unburned zone is written as

$$dE = dQ - pdV - h_a dm_a \tag{48}$$

The burning zone not only receives the mass from the air zone, but also there is an enthalpy flow from the fuel, which is ready to be burned in the time step. So, the first law of thermodynamics for the burning zone becomes

$$dE = dQ - pdV + h_a dm_a + h_f dm_f \tag{49}$$

The first law of thermodynamics for the combustion in time step dt is

$$f(E) = E(T_2) - E(T_1) - dQ + dW + dm_f Q_{vs} = 0 \tag{50}$$

If $f(E)$ is greater than the accuracy, the required new value of T_2 is calculated using the Newton–Raphson numerical method. The unburned zone temperature is calculated using the equation,

$$T_u = T_{soc}\left(\frac{P}{P_{soc}}\right)^{\gamma-1/\gamma} \tag{51}$$

3.2.2. Heat transfer model

The heat transfer between the cylinder trapped mass and the surrounding walls is calculated, using the formula of Annand [23]. The Annand formula to calculate the heat loss from the cylinder, is

$$dQ/dt = a\frac{\lambda_g}{D}(Re)^b\left(T_w - T_g\right) + c\cdot\left(T_w^4 - T_g^4\right) \tag{52}$$

In this equation 'T_w' is the cylinder wall temperature which is assumed as 450 K, and a, b, and c are constants. The constant values are taken as $a = 0.2626$, $b = 0.6$, $c = 5.67 * 10^{-8}$ W/m^2/K.

3.2.3. Ignition delay

The time delay between the start of injection and the start of combustion is defined as the ignition delay period [24]. The determination of the start of combustion (SOC) by selecting the proper method is a key issue in ignition delay studies. In the combustion model, the ignition delay is also taken into account. The ignition delay period is calculated by integrating Wolfer's relation, using the trapezoidal rule [25].

$$\int_{t_{inj}}^{t_{ign}} \frac{dt}{t(p,T)} = \frac{1}{K_{t_{inj}}}\int_{t_{inj}}^{t_{ign}} \frac{dt}{(p(t))^{-q}\exp\left(\frac{E}{RT(t)}\right)} = 1 \tag{53}$$

The values of various constants corresponding to a DI diesel engine are $K = 2272$; $q = -1.19$; $E/R = 4650$.

Where K = thermal conductivity, q = heat losses and E/R = activation energy/universal gas constant.

3.2.4. Wiebe's combustion model

The Wiebe function is used to predict the mass fraction burnt and the burn rate in IC engines, operating with different combustion systems and fuels. Wiebe linked the chain chemical reactions with the fuel reaction rate in IC engines and his approach is based on the premise that a simple one-step rate equation would not be adequate to describe the complex reacting systems, such as those occurring in an IC engine. The Wiebe functions [26] for the non-dimensional burn fraction x as a function of the degrees of crank angle can be written as

$$x = 1 - \exp\left[-6.908\left(\frac{\theta - \theta o}{\Delta\theta}\right)^{m+1}\right] \tag{54}$$

The heat release rate calculated with the help of the Wiebe function is,

$$\frac{dQ_c}{d\theta} = 6.908(m+1)\left(\frac{Q_{av}}{\Delta\theta}\right)\left(\frac{\theta - \theta_o}{\Delta\theta}\right)^m \exp\left[-6.908\left(\frac{\theta - \theta o}{\Delta\theta}\right)^{m+1}\right] \tag{55}$$

where x is the mass fraction burned, θ_o is the start of combustion and $\Delta\theta$ is the combustion duration. The parameter m represents the rate of combustion. Q_{av} is the heat released per cycle. The value of m for both the fuels is taken as 3.0. When calculating the heat release, prior knowledge of the actual overall equivalence ratio is necessary. The term equivalence ratio is defined as the ratio of the actual air–fuel ratio to the stoichiometric air–fuel ratio. This helps in fixing the mass of fuel to be admitted.

3.2.5. Chemistry of combustion

In a combustion process, the fuel and the oxidiser react to produce products of different compositions. The theory of combustion is a complex one, and has been the topic of intensive research for many years. Let us represent the chemical formula of a fuel as CαHβOγNδ. In the present case, it was considered that 10 species were present in the combustion product, and the combustion equation is given by:

$$\epsilon\varphi C\alpha H\beta O\gamma N\delta + 0.21O_2 + 0.79N_2 \rightarrow \nu 1CO_2 + \nu 2H_2O + \nu 3N_2 + \nu 4O_2 + \nu 5CO + \nu 6H_2 + \nu 7H + \nu 8O + \nu 9OH + \nu 10NO \quad (56)$$

From the atomic balance of each species C—H—O—N the following 4 equations, are obtained:

$$C \quad \epsilon\varphi\alpha = (y1 + y5)N1 \quad (57)$$

$$H \quad \epsilon\varphi\beta = (2y1 + 2y6 + y7 + y9)N1 \quad (58)$$

$$O \quad \epsilon\varphi\gamma + 0.42 = (2y1 + y2 + 2y4 + y5 + y8 + y9 + y10)N1 \quad (59)$$

$$N \quad \epsilon\varphi\delta + 1.58 = (2y3 + y10)N1 \quad (60)$$

The chemical reactions considered in equilibrium, are as follows:

$$0.5H_2 \longrightarrow H \quad (61)$$

$$0.5O_2 \longrightarrow O \quad (62)$$

$$0.5H_2 + 0.5O_2 \longrightarrow OH \quad (63)$$

$$0.5O_2 + 0.5N_2 \longrightarrow NO \quad (64)$$

$$H_2 + 0.5O_2 \longrightarrow H_2O \quad (65)$$

$$CO + 0.5O_2 \longrightarrow CO_2 \quad (66)$$

The use of the equilibrium constant is identical to maximising the entropy of the gas. This method is similar, when considering a restricted species list such as the present case [27]. Once the composition is known, the thermodynamic properties of interest such as enthalpy, entropy, specific volume and internal energy, can be computed.

3.2.6. Nitric oxide (NO) formation model

The current approach to model the NO_x emissions from diesel engines is, to use the extended Zeldovich thermal NO mechanism, by neglecting other sources of NOx formation. The extended Zeldovich mechanism consists of the following reactions:

$$O + N_2 \longrightarrow NO + N \quad (67)$$

$$N + O_2 \longrightarrow NO + O \quad (68)$$

$$N + OH \longrightarrow NO + H \quad (69)$$

This mechanism can be written as an explicit expression for the rate of change of the concentration of NO.

The change of NO concentration is expressed as follows:

$$(d\,(NO))/dt = 2(1 - \alpha^2)R_1/(1 + \alpha R_1/(R_2 + R_3)) \quad (70)$$

where R_i is the one-way equilibrium rate for the reaction i, defined as

$$R_1 = k_{1f}(N)e(NO)e, \quad R_2 = k_{2f}(N)e(O_2)e, \quad (71)$$

$$R_3 = k_{3f}(N)e(OH)e, \quad \alpha = (NO)/(NO)e \quad (72)$$

3.2.7. The net soot formation model

The exhaust of the CI engine contains solid carbon soot particles that are generated in the fuel rich regions inside the cylinder during combustion. Soot particles are clusters of solid carbon spheres, with the HC and traces of other components absorbed on the surface. They are generated in the combustion chamber in the fuel rich zones, where there is not enough oxygen to convert all the carbon to CO_2. Subsequently, as the turbulence motion continues to mix the components, most of these carbon particles find sufficient oxygen to react and form CO_2. Thus, soot particles are formed and consumed simultaneously in the combustion chamber.

The net soot formation rate was calculated by using the semi-empirical model proposed by Hiroyasu et al. [28]. According to this model, the soot formation rate (index *sf*) and soot oxidation rate (index *sc*) were given by

$$\frac{dm_{sf}}{dt} = A_{sf}\left(m_{f,ev} - m_{f,bu}\right)^{0.8} p^{0.5} \exp\left(-E_{sf}/R_{mol}T\right) \quad (73)$$

$$\frac{dm_{sf}}{dt} = A_{sc} m_{sn} (p_{o2}/p) p^{1.8} \exp\left(-E_{sc}/R_{mol}T\right) \quad (74)$$

where, the pressures are expressed in bar and d_{mf} is the unburned fuel mass in kg to be burned in time step dt. Therefore, the net soot formation rate is expressed as

$$\frac{dm_{sn}}{dt} = \frac{dm_{sf}}{dt} - \frac{dm_{sc}}{dt} \quad (75)$$

A computer program using MATLAB was generated, with all the abovementioned equations and considering all the values of the constants, in order to predict the combustion attributes, such as the in-cylinder pressure, crank angle, heat release rate, heat losses and the NO emissions.

4. Results and discussion

4.1. Spray profile of diesel and BMDE15

In a CI engine, once the fuel is injected into the compressed air stream in the cylinder, the fuel jet disintegrates into a core of fuel surrounded by the spray envelope of air and fuel particles. The spray envelope is created both by the atomisation and by the vapourisation of the fuel. The turbulence of air in the combustion chamber passing across the jet tears the fuel particles from the core. A mixture of air and fuel is found at some location in the spray envelope and the oxidation starts. Thus, the study of formation of spray is important for any diesel fuel, when it is used in a diesel engine. In this study, the fuel spray patterns for diesel and the BMDE15 emulsion are obtained using the MATLAB program. Fig. 2(a) and (b) shows the spray profile of diesel and BMDE15 respectively at full load.

It can be observed from both the figures, that near the nozzle exit the spray is narrow and further downstream at the region of the spray body the spray widens, because of the droplet breakup and collision phenomena and the interaction with the induced gas flow field. Chemical properties such as density, viscosity and surface tension will affect the spray angle. Diesel has higher density and viscosity in comparison with the BMDE15 emulsion. However, when surface tension is low, spray droplet is prone to quickly break-up and wider dispersion and cause a relatively larger spray droplet. It is apparent from Fig. 2(a) and (b) that BMDE15 has a smaller cone angle with high penetration which may be due to the combined effects of density, viscosity and surface tension.

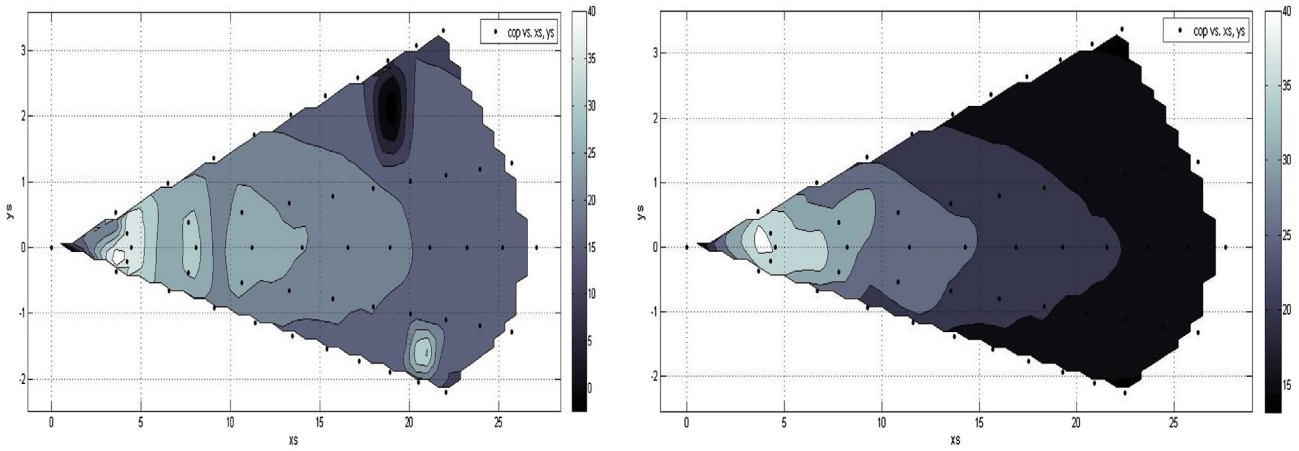

Figure 2 (a) Diesel spray and (b) BMDE15 emulsion spray.

4.2. Combustion parameters

4.2.1. Cylinder pressure

Fig. 3 depicts the experimental and simulated results of the diesel engines fuelled with diesel and BMDE15, at full load.

The simulated results of both the test fuels gave higher values compared to the experimental results. The lower cylinder pressure for the experimental results may be due to the instruments' error, and physical condition during the experiments and the uncertainty of the data. It is apparent from the figure that the ignition of diesel is the earliest for the simulated results followed by its experimental results, the BMDE15 simulated results, and finally, the BMDE15 experimental results. The peak cylinder pressure of a CI is predominantly influenced by the ignition delay, the amount of fuel burnt in the initial stage of fuel combustion and the mixture formation in the delay period. The peak cylinder pressure for the BMDE15 is found to be the highest, followed by the BMDE15 experimental results, diesel simulated and experimental results. The difference in the peak cylinder pressure of BMDE15 between the simulated and experimental results is about 3%. The peak pressure is shifted away from the top dead centre by about 5–7 °CA. In the case of diesel, the peak cylinder pressure for the simulated and experimental results is about 75–70.6 bar which is attained close to the TDC. The peak cylinder pressures of BMDE15 operation, both in the simulated and experimental results, are higher than those of diesel operation, due to longer ignition delay and better fuel mixture formation, that results in more complete combustion. The deviation between the simulated and the experimental results for diesel and BMDE15 is about 2–4 °CA respectively.

4.2.2. Ignition delay

Fig. 4 illustrates the variation of ignition delay at different loads for diesel and BMDE15 operations. Ignition delay is the time difference measured in crank angle between the start of injection and start of combustion [25]. It is evident from the figure, that the simulated and the experimental results for the ignition delay for the diesel and BMDE15 operations follow a similar trend. The ignition delay increases with the increase in the load as a result of the increase in the cylinder gas temperature. The ignition delay is found to be longer for the simulated and experimental results for the BMDE15 operation than those of diesel operation. It can be observed from the figure, that there is about 5–10 °CA deviation in the ignition

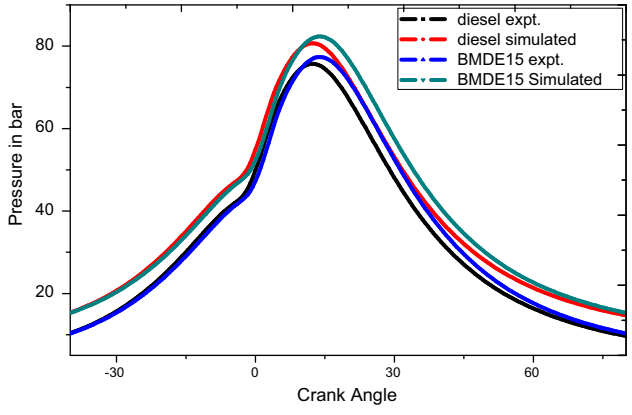

Figure 3 Cylinder pressure with crank angle for diesel and BMDE15.

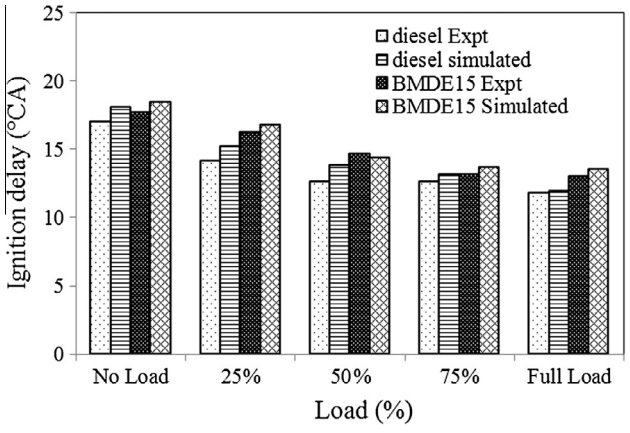

Figure 4 Variation of ignition delay with load.

delay period of experimental and theoretical results for both the fuels. The ignition delay depends upon the pressure, temperature, fuel and air mixture, equivalence ratio, flame speed, etc. During the engine operating condition, the cylinder wall temperature may increase the fuel temperature. So, the chemical reaction period may be accelerated; hence, the delay period is shortened compared to the theoretical result. Also, the ignition delay period may decrease in the lean and rich mixture zones.

The calculated values for the ignition delay in the BMDE15 operation are higher than those of diesel values, which is due to the influence of the temperature, pressure and the time of injection. The longer ignition delay of the BMDE15 operation than that of diesel operation throughout the load spectrum, is due to the lower cetane number of BMDE15.

4.3. Emission parameters

4.3.1. NO emission

In a CI engine, the NO_x emission is one of the major pollutants and is predominantly influenced by the amount of oxygen available, and the in-cylinder temperature [26]. The NO_x emission is composed of NO, NO_2, N_2O, N_2O_5, NO_3. Nitric oxide is the major constituent and NO_2 is a minor constituent, while the others are negligible. At elevated temperatures (i.e.) above 1500 °C, N_2 can react with O_2 faster and may result in more NO_x emission. As CI engines have a higher compression ratio and are lean burn engines, the peak temperature is well above 1500 °C; hence, there is a higher NO_x formation. The comparison between the simulated and experimental results for NO emission from diesel and BMDE15 operations is shown in Fig. 5. The brake specific NO emissions are obtained from the simulation and experiments for both diesel and BMDE15, show a declining trend as the load increases. This is because of the increase in the load which is a denominator for the calculation of NO. The NO emission values obtained from the simulation and experiments are found to be lower than those of diesel operation, because of the high latent heat of the vapourisation of BMDE15.

An overall marginal deviation of 2–1% is noticed between the simulation and experimental results of the NO emission values in diesel operation from no load to full load, while the deviation is 2–1% from no load to full load in the BMDE15 operation.

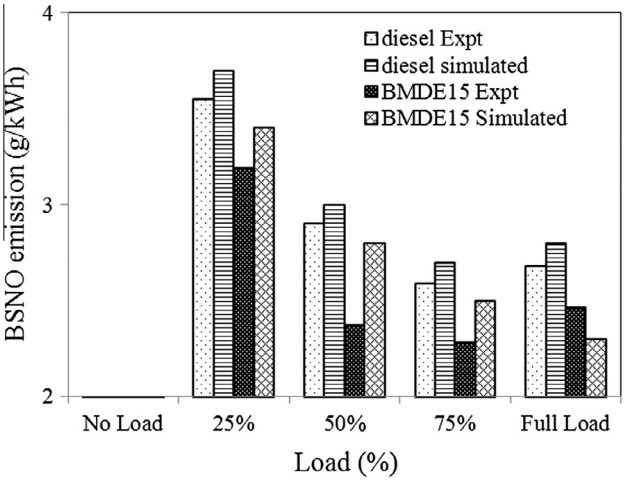

Figure 5 Variation of BSNO emission with load.

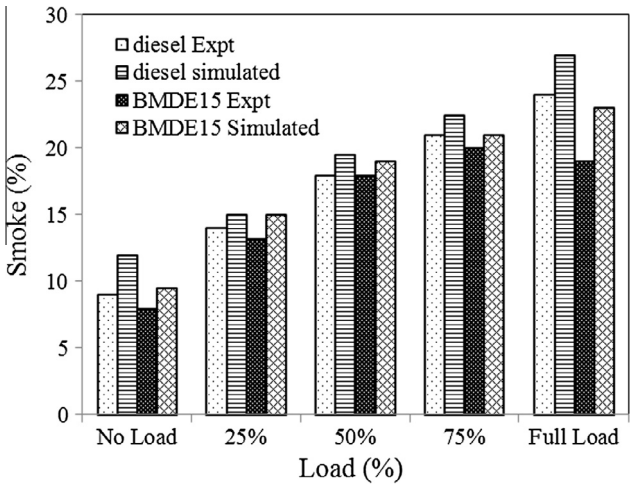

Figure 6 Variation of smoke with load.

4.3.2. Smoke

The variation of the simulated and experimental results of smoke emission for diesel and BMDE15 is shown in Fig. 6. The simulated results of diesel for smoke emission are found to be high compared to the experimental results of diesel and the simulated and experimental results of BMDE15. The smoke emission is a result of the oxygen unavailability in the diffusion combustion phase, use of high molecular weight fuel and the aromatic content of fuel [29]. Diesel has a high carbon to hydrogen ratio, high molecular weight, less oxygen and high aromatic content [30]. Hence, higher smoke emission is observed with the diesel operation compared to that of BMDE15 operation.

The deviation between the simulated and experimental values of diesel and BMDE15 is about 3% and 4% respectively, at full load.

5. Conclusion

A comprehensive two zone model was developed to validate the experimental results that were obtained from a single cylinder, four stroke, air cooled, DI diesel engine run on two different fuels, viz., diesel and BMDE15.

The following is the summary of the results:

- The spray pattern of BMDE15 is found to be better compared to that of diesel. The better atomisation and vapourisation of fuel is achieved with BMDE15 due to its lower density.
- The experimental and simulated results show that the peak cylinder pressure of the BMDE15 is found to be marginally higher than that of diesel at full load. The deviation between the simulated and the experimental results for the diesel operation at full load is about 5%. In the case of the BMDE15 operation, the deviation is about 3% at full load.

- The ignition delay of BMDE15 is found to be longer than that of diesel in the entire engine operation. The values of ignition delay obtained in the experimentation for both the fuels are close to the values obtained by simulation.
  - The NO emission of the engine run on the BMDE15 emulsion is found to be lower than that of diesel which is due to the high latent heat of vapourisation. This is validated with the NO emission model. The deviation between the simulated and experimental results for the diesel and BMDE15 operations is about 7.1% and 5% respectively, at full load.
  - The smoke opacity is found to be lower for the BMDE15 operation compared to that of diesel. The smoke opacity of BMDE15 obtained by simulation is higher by about 4% than that of the experiment.

Acknowledgements

This paper has been elaborated in the framework of the project New creative teams in priorities of scientific research, reg. no. CZ.1.07/2.3.00/30.0055, supported by Operational Programme Education for Competitiveness and co-financed by the European Social Fund and the state budget of the Czech Republic. The authors also thank the National Institute of Technology, Rourkela for providing test facilities for carrying out the research work.

References

[1] R.C.C. Leite, M.R.L.V. Leal, L.A.B. Cortez, L.A. Barbosa, W. M. Griffin, M.I.G. Scandiffio, Can Brazil replace 5% of the 2025 gasoline world demand with ethanol?, Energy 34 (2009) 655–661
[2] A. Demirbas, Bioethanol from cellulosic materials: a renewable motor fuel from biomass, Energy Sources 27 (2005) 327–337.
[3] B. Hahn-Hägerdal, M. Galbe, M.F. Gorwa-Grauslund, G. Lidén, G. Zacchi, Bio-ethanol-the fuel of tomorrow from the residues of today, Trends Biotechnol. 24 (2006) 549–556.
[4] E.E. Ecklund, R.L. Bechtold, T.J. Timbario, P.W. McCallum, State-of-the-art Report on the use of Alcohols in Diesel Engines, SAE Technical Paper 840118, 1984, pp. 1684–1702.
[5] R.D. Reitz, F.V. Bracco, On the Dependence of Spray Angle and other Spray Parameters on Nozzle Design and Operating Conditions, SAE Technical Paper No. 790494, 1979.
[6] Sanjay Patil, Thermodynamic modelling for performance analysis of compression ignition engine fuelled with biodiesel and its blends with diesel, Int. J. Recent Technol. Eng. (IJRTE) 1 (2013) 134–138.
[7] S. Awad, E.G. Varuvel, K. Loubar, M. Tazerout, Single zone combustion modeling of biodiesel from wastes in diesel engine, Fuel 106 (2013) 558–568.
[8] D.C. Rakopoulos, C.D. Rakopoulos, E.G. Giakoumis, R.G. Papagiannakis, D.C. Kyritsis, Experimental-stochastic investigation of the combustion cyclic variability in HSDI diesel engine using ethanol–diesel fuel blends, Fuel 87 (2008) 1478–1491.
[9] C.D. Rakopoulos, D.C. Rakopoulos, D.C. Kyritsis, Development and validation of a comprehensive two-zone model for combustion and emissions formation in a DI diesel engine, Energy Resour. 27 (2003) 1221–1249.
[10] Dohoy Jung, Dennis N. Assanis, Multi-zone DI Diesel Spray Combustion Model for Cycle Simulation Studies of Engine Performance and Emissions, SAE Paper No. 2001-01-1246.
[11] Paramust Juntarakod, A quasi-dimensional three-zone combustion model of the diesel engine to calculate performances and emission using the diesel–ethanol dual fuel, Contemp. Eng. Sci. 7 (1) (2014) 19–37.
[12] C.D. Rakopoulos, K.A. Antonopoulos, D.C. Rakopoulos, Multi-zone modeling of diesel engine fuel spray development with vegetable oil, bio-diesel or diesel fuels, Energy Convers. Manage. 47 (2006) 1550–1573.
[13] C.D. Rakopoulos, G.M. Kosmadakis, E.G. Pariotis, Critical evaluation of current heat transfer models used in CFD in-cylinder engine simulations and establishment of a comprehensive wall-function formulation, Appl. Energy 87 (2010) 1612–1630.
[14] C.A. Harch, M.G. Rasul, N.M.S. Hassan, M.M.K. Bhuiya, Modelling of engine performance fuelled with second generation biodiesel, Proc. Eng. 90 (2014) 459–465.
[15] P. Ottikkutti, J.V. Gerpen, K.R. Cui, Multizone Modeling of a Fumigated Diesel Engine, SAE, 1991, pp. 1–21.
[16] J.I. Ramos, Internal Combustion Engine Modeling, Hemisphere Publishing Corporation, New York, 1989.
[17] Z. Sahin, O. Durgun, Multi-zone combustion modeling for the prediction of diesel engine cycles and engine performance parameters, Appl. Therm. Eng. 28 (2008) 2245–2256.
[18] Dulari Hansdah, S. Murugan, L.M. Das, Experimental studies on a DI diesel engine fueled with bioethanol–diesel emulsions, Alexandria Eng. J. (52) (2013) 267–276.
[19] M. Arai, M. Tabata, H. Hiroyasu, M. Shimizu, Disintegration Process and Spray Characterization of Fuel Jet Injected by a Diesel Nozzle, SAE Technical Paper No. 840275, 1984.
[20] J.C. Dent, J.A. Derham, Air motion in a four-stroke direct injection diesel engine, Proc. Inst. Mech. Eng. 188 (1974) 269–280.
[21] C.D. Rakopoulos, D.C. Rakopoulos, D.C. Kyritsis, Development and validation of a comprehensive two-zone model for combustion and emissions formation in a DI diesel engine, Energy Resour. 27 (2003) 1221–1249.
[22] A.S. Ramadhas, S. Jayaraj, C. Muraleedharan, Theoretical modeling and experimental studies on biodiesel-fueled engine – technical note, Renew. Energy 31 (2006) 1813–1826.
[23] W.J.D. Annand, Heat transfer in the cylinders of reciprocating internal combustion engines, Proc. Inst. Mech. Eng. 177 (1963) 973–990.
[24] Heywood, Internal Combustion Engines Fundamentals, McGraw Hill Publications, 1988, pp. 491–667.
[25] N.D. Whitehouse, R.J.B. Way, A Simple Method for the Calculation of Heat Release Rates in Diesel Engines based on the Fuel Injection Rate, SAE Technical Paper No. 710134, 1971.
[26] R.J.B. Way, Methods for determination of composition and thermodynamic properties of combustion products for internal combustion engine calculations, Proc. Inst. Mech. Eng. 190 (60/76) (1977) 687–697.
[27] T.K. Gogoi, D.C. Baruah, A cycle simulation model for predicting the performance of a diesel engine fuelled by diesel and biodiesel blends, Energy 35 (2010) 1317–1323.
[28] H. Hiroyasu, T. Kadota, M. Arai, Development and use of a spray combustion modeling to predict diesel engine efficiency and pollutant emissions, Bull Jpn. Soc. Mech. Eng. 26 (214) (1983) 569.
[29] Dulari Hansdah, Experimental Studies of Bioethanol Fueled DI Diesel Engine using Different Techniques, Ph.D. Thesis, NIT Rourkela, 2014.
[30] V. Ganesan, Computer Simulation of Compression Ignition Engine Processes, University Press(India) Ltd., Hyderabad, India, 2000.